Journal of the Operations Research Society of Japan
Vol. 60, No. 3, July 2017, pp. 400–417

GEOMETRIC PROBABILITY MODELS TO ANALYZE STRATEGIES FOR FINDING A BURIED CABLE

Ken-ichi Tanaka Kana Shiina
Keio University

(Received March 31, 2016; Revised January 21, 2017)

Abstract Different strategies can be used to find a straight cable buried underground. The original problem considered by Faber et al. focused on a telephone company that wishes to dig a trench to locate a straight cable. The cable is known to pass within a given distance, a, from a marker erected above the putative location of the cable. Faber et al. showed that the shortest simply connected curve guaranteed to find the cable is a U-shaped curve whose length is about 18% less than that of a circular trench of radius a. This problem can be regarded as minimizing the maximum length that a trench digger must dig. In reality, once the cable is found, digging can stop. So far, however, no attempt has been made to evaluate the trench shape on characteristics other than the maximum trench length. In this paper, we present geometric probability models to analytically derive the distribution of trench length and calculate the expected value and variance for both the short-length (U-shaped) trench and a circular trench. Our main result is that the expected digging length is about 5% less for the circular trench than for the U-shaped trench.

Keywords: Applied probability, beam detector, geometric probability, digging length distribution, urban infrastructure, urban operations research

1. Introduction

Faber et al. [4, 5] considered strategies for finding a straight cable buried underground by digging a trench, finding the maximum length necessary to guarantee discovery of a straight cable known to be buried within a units from a given marker. In this paper, geometric probability models are presented to analyze expected length and variance of various shapes of trench.

In the original formulation, the problem considers the length of the trench that guarantees locating a cable while digging near it. In other words, it focuses on the maximum trench length that a trench digger would need to dig before finding the cable. Of course, a circular trench of radius a centered at the maker would guarantee this, but it is known that more efficient shapes of trench exist. One such example is the U-shaped trench shown in Figure 1 (b), composed of a semicircle and two line segments of length a, where a is the radius of the semicircle. Faber et al. [4] proved the very interesting fact that, among simply connected curves that ensure finding a cable, the U-shaped trench is the best in terms of minimizing the maximum total trench length. This U-shaped trench, with length $(\pi + 2)a \approx 5.14a$, is about 18% shorter than the circular trench, with length $2\pi a \approx 6.28a$. Focusing on this aspect, the existing literatures argue that U-shaped trench is 18% better than the circular trench.

While the above result is interesting mathematically, the maximum trench length is only one of many indices that are important in real applications. So far however, to our knowledge, no attempt has been made to evaluate the trench shape on the basis of measures other than the maximum necessary trench length. Since a trench digger can stop digging

once a cable is found, the expected trench length before a trench digger locates a cable may be more important.

In this paper, we focus on two strategies for finding a cable: digging along the circumference of the circular trench, and digging the U-shaped trench described above. We analytically derive the distributions of trench length with stopping on discovery for the two models and compute the expected values of trench length and their variances. This approach allows us to evaluate the two strategies more broadly than when only the maximum trench lengths are available.

To derive the trench length distribution, a probabilistic approach is necessary. We develop geometric probability models that describe how each possible position of a cable occurs relative to the marker, using random lines. One of our main results is that, in terms of the expected trench length, the circular trench is superior to the U-shaped trench.

The remainder of this paper is organized as follows. In the next section, we introduce some related literature. In Section 3, we discuss general assumptions and describe the problem. We then focus on the circular trench (O-model) and derive the cumulative distribution function (cdf) of trench length in Section 4. From the cdf, we analytically obtain the probability density function (pdf) of trench length and the corresponding expected value and variance. We show that the pdf is obtained as the cosine curve, and this simplicity allows us to analytically derive several other indices. Next, in Section 5, we investigate the U-shaped trench (U-model). Although the analysis is much more complicated than that for the O-model, we analytically obtain the cdf and pdf of the U-model. In Section 6, we compare characteristics of the two strategies for finding a cable. One of our main results is that, in terms of expected trench length, the circular trench is about 5% superior to the U-shaped trench. In Section 7, we conclude the paper and present several important directions for future research.

2. Literature Review

Croft [1] considered the problem of finding the shortest continuous curve in the plane that intercepts every chord of a fixed disk of unit radius. There are several variants of this problem, differing according to which of the following curves (or sets of curves) are allowed: (a) a single continuous (rectifiable) curve; (b) a countable collection of rectifiable curves somehow connected to each other; and (c) a countable collection of rectifiable curves not necessarily connected to each other [2]. Croft conjectured that for cases (a) and (b), the U-shape is the shortest curve, with length of $\pi + 2 \approx 5.142$ [1]. For case (a), this conjecture was proven by Faber et al. [4]. For case (c), which relaxes the connectivity assumption, the length can be reduced substantially. The best known 2- and 3-curve connected sets have lengths about 4.819 and about 4.800, respectively (see for example [6]).

Similar problems can be defined for an arbitrary convex region K instead of the unit circle. Faber et al. [5] give short curves in cases (a), (b), and (c) for various convex sets K, in particular, for regular n-gons with $n = 3$, 4, 5, and 6.

Problems of this type, while simple and easily understandable, are often very hard to solve. For example, when K is a unit square, the lengths of the shortest curve for (a) and (b) are known to be 3 and $1 + \sqrt{3} \approx 2.732$, respectively. However, these two cases correspond to particular instances of well-known classical problems with nodes taken from four vertices of a unit square: the former is an instance of the minimum spanning tree problem, and the latter is the geometric Steiner tree problem. In contrast, for case (c), the best known 2-curve connected set has length $\sqrt{2} + \frac{\sqrt{6}}{2} \approx 2.639$. However, a proof of the optimality of

this result has not yet been given.

A curve that intercepts all lines intersecting a given convex polygon is also called a *beam detector* [6]. This is because the lines can be considered as beams, and curves that intersect every such line can be seen as a detector for beams. The word *barrier* is also used with the same meaning [3]. *Opaque set* is another term with a similar meaning. Algorithms for finding a short *opaque set* have been developed, such as that in [3].

There are several variants of the beam detection problem. Examples include the problems of finding land for a swimmer lost in a dense fog in a river or the sea. A similar example is finding a straight road when lost in a forest. These and other types of variants can be found in [2, 6–8, 10].

As introduced in the previous section, the problem can be seen as finding a trench that ensures finding an underground cable during digging of the trench [5]. A similar situation was treated by Stewart [14], in which Sherlock Holmes has to find an underground tunnel as quickly as possible. The only way to find the underground tunnel that runs through straight in a court was to dig a trench. The U-shaped trench was introduced as the most efficient shape to find the tunnel.

The trench-digging application has an additional aspect not considered in beam detector applications. In digging a trench, the time to find a cable depends on the location in which the cable is found. In the literature, however, this important aspect has not yet been sufficiently examined. Earlier studies evaluate the efficiency of curves exclusively on the basis of the maximum length a trench digger might need to dig [5].

Since the problem involves geometrical and spatial aspects, the proposed probabilistic models use some basic concepts of geometric probability. Geometric probability has been applied to a variety of problems that treat distribution of objects in space [11–13]. These approaches are useful in various fields, including astronomy, biology, crystallography, forestry, and search theory. In this paper, we employ random lines to model the realization of a random cable relative to the marker.

In the field of geometric probability, problems dealing with random chords in a circle have been extensively studied. Distributions of chord length and their expected values have been calculated under several different generation rules for random chords (see for example [11, 13]). While the situation we assume in modeling a random cable is similar to those assumed in the above studies, distributions of trench length that a trench digger has to search before identifying a cable have not been treated so far.

Geometric probability has also been applied to evaluating urban service systems [9, 15, 16]. For example, the distribution of distance from uniformly distributed points in a given region to a facility fixed at a given point in the region has been derived. Also, by assuming travel patterns in an urban area, the distribution of distances between various pairs of points within a region has been calculated. These results have been summarized in [9, 15, 16]. The proposed models can be seen as new geometric probability models arising in urban applications.

3. Problem Description

This section explains the general situation and presents basic assumptions. We assume that the relative position of the cable from the marker is unknown, but it is always within a units of the marker. This paper focuses on two methods of finding a cable: one is to dig along the circumference of the circle of radius a centered at the marker (the O-method), the other is to dig along the U-shaped curve with the center of the semicircle at the marker

(the U-method).

From the literature it is known that the U-shaped curve, with total length $(\pi + 2)a$, is the shortest simply connected curve that ensures finding a cable. This can be seen as saying that, in terms of the maximum trench length, the U-shaped curve is optimal. Our focus of this paper is to compare the two methods from a different viewpoint, by deriving the pdfs of the trench lengths for both models.

In this paper, the path of the trench must be simply connected at all times. In other words, a trench digger continuously digs along a given curve without interruption. For the U-method, this assumption allows a trench digger to start finding the cable only from one endpoint of the "U", moving toward the other endpoint. Relaxation of this assumption is an interesting future topic, which we discuss in the final section.

As shown in Figure 1, we introduce an x-y coordinate system with the marker at the origin for both models. The position of a cable is represented by the distance p between the marker and the cable, and the angle θ that the perpendicular to the cable makes with the x-axis. A probabilistic approach is necessary to derive the pdf of the trench length, unlike in previous studies that focus solely on the maximum value needed to ensure discovery. We construct probabilistic models by assuming that p and θ are random variables. Throughout the paper, we assume that p and θ are independent and that θ is uniformly distributed in the range $[0, 2\pi]$.

With this assumption, we can consider, without loss of generality, that a trench digger starts checking a cable from $(a, 0)$ in the counter-clockwise direction along the circumference of the circle of radius a. Also for the U-shape, we can focus on the situation where a trench digger starts checking from (a, a) and moves toward the other end of the U-shape at $(a, -a)$.

The joint pdf of θ and p is denoted by $f_{\Theta,P}(\theta, p)$. In this paper, we formulate a method to derive the cdfs and the pdfs of the trench length for the O-model and U-model, assuming that θ and p are independent and θ is uniformly distributed in the range $\theta \in [0, 2\pi]$:

$$f_{\Theta,P}(\theta, p) = \frac{1}{2\pi} f_P(p), \quad (\theta, p) \in R, \tag{3.1}$$

where $R = [0, 2\pi] \times [0, a]$. Based on the method, we explicitly derive the cdfs and the pdfs of the trench length for both models in the most important case where θ and p are independent and uniformly distributed in the ranges $\theta \in [0, 2\pi]$ and $p \in [0, a]$:

$$f_{\Theta,P}(\theta, p) = \frac{1}{2\pi a}, \quad (\theta, p) \in R. \tag{3.2}$$

4. Trench Length Distribution: O-model

This section focuses on the O-model. We derive the cumulative distribution function (cdf) of the trench length L_{O}, which gives important measures such as the pdf and the expected trench length. The analysis proceeds as follows.

(i) Divide the points in $(\theta, p) \in R$ into sub-regions, each having the same intersection pattern between a cable and the circumference of the circle;

(ii) For each sub-region specified in (i), express the trench length as a function of θ and p;

(iii) For an arbitrary trench length $l \in [0, 2\pi a]$, identify the set of points $\Omega_{\mathrm{O}}(l)$ where the trench length L_{O} is less than or equal to l;

(iv) Integrate $f_{\Theta,P}(\theta, p)$, the joint density function of θ and p, over $\Omega_{\mathrm{O}}(l)$ to obtain $F_{L_{\mathrm{O}}}(l)$, the cdf of L_{O};

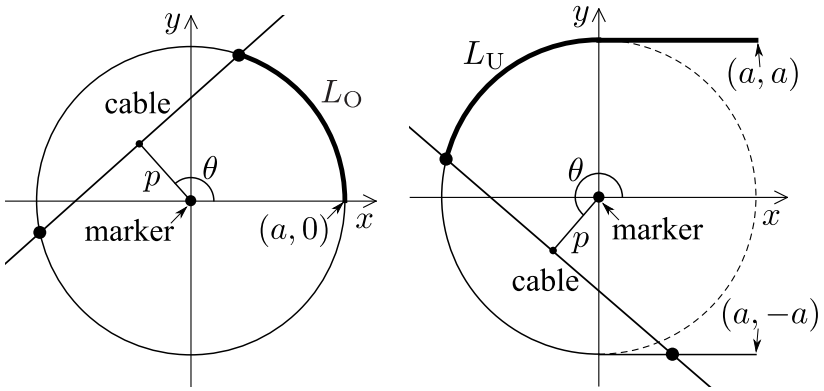

(a) O-model (b) U-model

Figure 1: The situation for O- and U-models

(v) Obtain $f_{L_O}(l)$ (the pdf of L_O) and the expected trench length and its variance.

Figure 2 shows the possible patterns of intersections between a cable and the circumference of the circle. There are three cases: (A), (B), and (C). In the case of the O-model, the cable always intersects the circle at two points, except the case of measure zero (i.e., when the cable is a units from the origin), where the cable lies tangent to the circle. To express L_O as a function of θ and p, we need to identify which of the two intersection points the trench digger first locates while digging a trench starting from $(a, 0)$. In Figure 2, the two intersection points are indicated as black dots and the path of circular arc along which the trench digger proceeds is illustrated by thick black arc. Let us denote the angle corresponding to the thick black arc for the three cases as φ_A for (A), φ_B for (B), and φ_C for (C). These three angles can be written as follows:

$$\varphi_A = \theta + \arccos\frac{p}{a}, \tag{4.1}$$

$$\varphi_B = \theta - \arccos\frac{p}{a}, \tag{4.2}$$

$$\varphi_C = \arccos\frac{p}{a} - (2\pi - \theta). \tag{4.3}$$

Figure 3 illustrates how to identify each sub-region over $R = [0, 2\pi] \times [0, a]$ in which the three patterns (A), (B), and (C) are realized. Figures 3 (a), 3 (b) and 3 (c) correspond to the case for $0 \le \theta \le \frac{\pi}{2}$, $\frac{\pi}{2} \le \theta \le \frac{3\pi}{2}$ and $\frac{3\pi}{2} \le \theta \le 2\pi$, respectively. The dashed line shows the cable that passes through $(a, 0)$. The black dot is the intersection point found by the trench digger, and the gray dot is the other intersection point. As can be seen from Figures 3 (a) and 3 (c), the expression for L_O changes depending on whether the value of p is larger than or smaller than $a\cos\theta$. Figure 3 (a) shows the threshold value of p between case (A) and case (B); Figure 3 (c) shows the threshold value of p between case (C) and case (B). As can be seen in Figure 3 (b), when $\frac{\pi}{2} \le \theta \le \frac{3\pi}{2}$ the intersection pattern is always the same: case (B).

We can summarize the division of R into a set of sub-regions according to intersection pattern as shown in Figure 4.

By Equations (4.1)–(4.3), the trench length L_O can be expressed as follows:

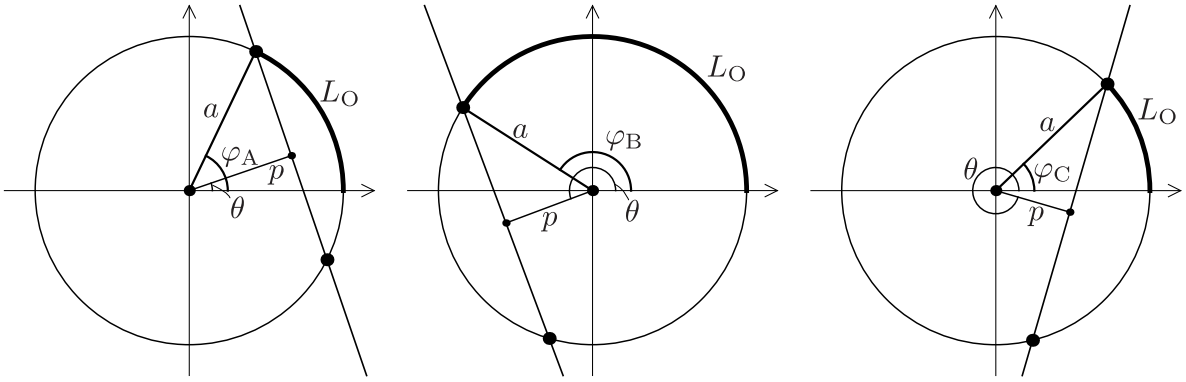

(a) region (A) (b) region (B) (c) region (C)

Figure 2: Intersection patterns of a cable and the circle (O-model)

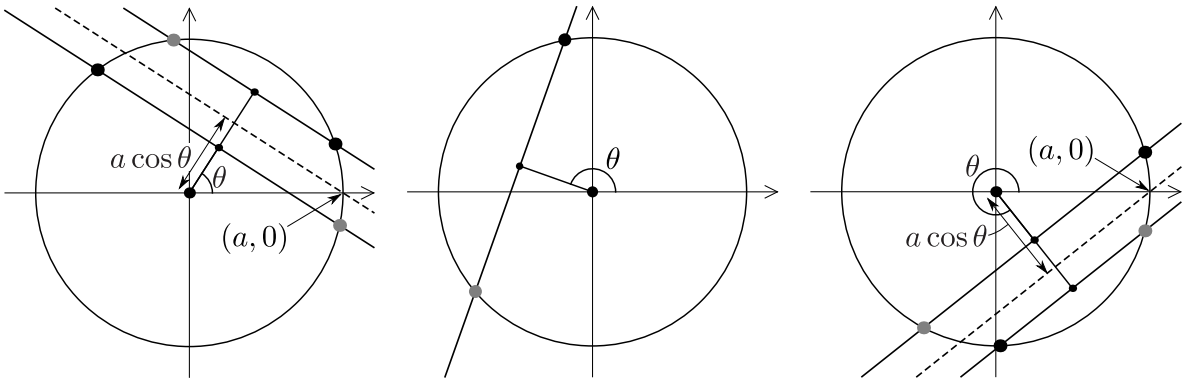

(a) $0 \le \theta \le \frac{\pi}{2}$ (b) $\frac{\pi}{2} \le \theta \le \frac{3\pi}{2}$ (c) $\frac{3\pi}{2} \le \theta \le 2\pi$

Figure 3: Illustration of changes of patterns

(i) (A)

$$L_{\mathrm{O}} = a\left(\theta + \arccos\frac{p}{a}\right), \tag{4.4}$$

(ii) (B)

$$L_{\mathrm{O}} = a\left(\theta - \arccos\frac{p}{a}\right), \tag{4.5}$$

(iii) (C)

$$L_{\mathrm{O}} = a\left(\arccos\frac{p}{a} - (2\pi - \theta)\right). \tag{4.6}$$

To derive the cdf of the trench length, $F_{L_{\mathrm{O}}}(l)$, we have to identify the region $\Omega_{\mathrm{O}}(l)$ in R that satisfies the condition $L_{\mathrm{O}} \le l$. Using the notation, $F_{L_{\mathrm{O}}}(l)$ can be expressed as follows:

$$F_{L_{\mathrm{O}}}(l) = \iint_{\Omega_{\mathrm{O}}(l)} f_{\Theta,P}(\theta, p)\mathrm{d}\theta\mathrm{d}p. \tag{4.7}$$

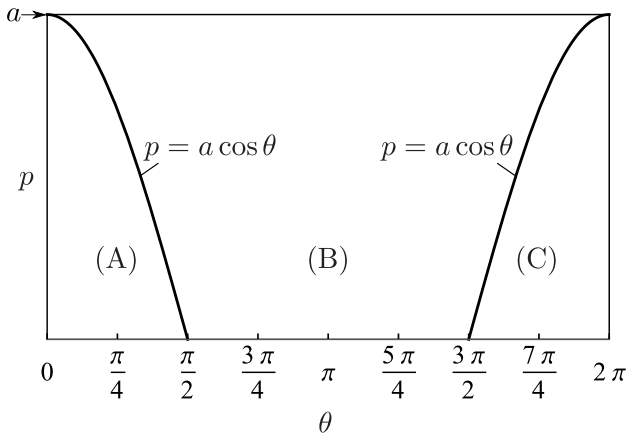

Figure 4: Division of R into sub-regions by intersection pattern (O-model)

It should be noted that the shape of $\Omega_{\mathrm{O}}(l)$ changes depending on the value of l, where $l \in [0, 2\pi a]$. For more detailed process for deriving the cdf, see the appendix A.

Under the assumption of Equation (3.2), the cdf can be derived as follows:

$$F_{L_{\mathrm{O}}}(l) = \frac{l}{2\pi a} + \frac{1}{\pi} \sin\left(\frac{l}{2a}\right), \quad (0 \le l \le 2\pi a). \tag{4.8}$$

As Equation (4.8) shows, the cdf can be expressed in the same form for all values of $l \in [0, 2\pi a]$. By differentiating Equation (4.8) with respect to l, the pdf of trench length $f_{L_{\mathrm{O}}}(l)$ can be obtained as follows:

$$f_{L_{\mathrm{O}}}(l) = \frac{1}{2\pi a} + \frac{1}{2\pi a} \cos\left(\frac{l}{2a}\right), \quad (0 \le l \le 2\pi a). \tag{4.9}$$

As can be seen from Equation (4.9), $f_{L_{\mathrm{O}}}(l)$ is a very simple cosine curve plus a constant value. Because of this simplicity, we can easily calculate important measures from the pdf. From Equation (4.9), the expected value of the trench length and the variance can be derived as follows:

$$\mathrm{E}[L_{\mathrm{O}}] = \int_0^{2\pi a} l f_{L_{\mathrm{O}}}(l) \mathrm{d}l = \frac{\pi^2 - 4}{\pi} a \approx 1.868a, \tag{4.10}$$

$$\mathrm{Var}[L_{\mathrm{O}}] = \int_0^{2\pi a} \left(l - \mathrm{E}[L_{\mathrm{O}}]\right)^2 f_{L_{\mathrm{O}}}(l) \mathrm{d}l = \frac{\pi^4 - 48}{3\pi^2} a^2 \approx 1.669a^2. \tag{4.11}$$

Figure 5 illustrates the trench length corresponding to the expected length. The angle from the marker is about 107°. It is worthwhile to point out that this value is less than one third of the maximum value of 360°.

5. Trench Length Distribution: U-model

This section focuses on the U-model and derives the cdf of the trench length. The procedure for deriving the cdf is similar to that for the O-model, except that the process is much more complicated due to the lower symmetry of the U-model. The analysis proceeds as follows.

(i) Divide the points in $(\theta, p) \in R$ into sub-regions with each having the same intersection pattern between a cable and the U-shape;

(ii) For each sub-region specified in (i), express the trench length as a function of θ and p;

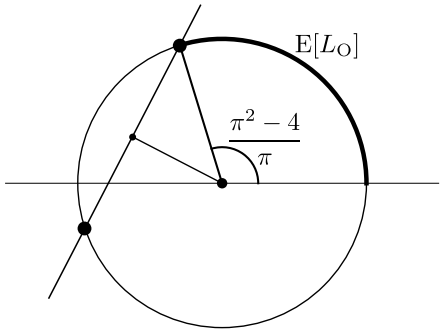

Figure 5: Expected value of trench length for O-model

(iii) For an arbitrary trench length $l \in [0, (\pi+2)a]$, identify the set of points $\Omega_{\mathrm{U}}(l)$ where the trench length L_{U} is less than or equal to l;

(iv) Integrate $f_{\Theta,P}(\theta, p)$, the joint density function of θ and p, over $\Omega_{\mathrm{U}}(l)$ to obtain $F_{L_{\mathrm{U}}}(l)$, the cdf of L_{U};

(v) Obtain $f_{L_{\mathrm{U}}}(l)$ (the pdf of L_{U}) and the expected trench length and its variance.

Unlike in the O-model, there are some cases in which only one intersection point occurs between a cable and the U-shaped trench. It should be noted that although we need to know only the point where the trench digger finds the cable in order to derive the cdf of the trench length, it is valuable to identify both intersection points (when there are two such points) to formulate variants of the proposed model.

Figure 6 illustrates all the intersection patterns between a cable and the U-shape. In the figure, black dots illustrate intersection points, and thick lines indicate the path of trench digging. For the U-model, 11 different intersection patterns occur, labeled (A) through (K). For cases (B), (D), (H), and (J), there is only one intersection point; other cases have two intersection points.

Figure 7 shows all 11 sub-regions in the region R. Sub-regions change at the following four curve sections:

$$p = a\sin\theta, \tag{5.1}$$

$$p = -a\sin\theta, \tag{5.2}$$

$$p = a(\cos\theta - \sin\theta), \tag{5.3}$$

$$p = a(\cos\theta + \sin\theta). \tag{5.4}$$

For each sub-region, the intersection point(s) are labeled by S_1(initial segment), S_2(terminal segment), C(semicircle) or two of these three. For example, sub-region (E) has two labels S_1 and C, which indicates a cable intersects the U-shaped trench at S_1 and C. Also the point a trench digger finds is the one shown in the upper location, S_1 in the case of sub-region (E).

To express L_{U} as a function of (θ, p), coordinates for all intersection points that a trench digger finds while digging from (a, a) along the U-shape have to be identified. There are four different expressions for the coordinate of intersection points: two for the semicircle, one for the initial segment S_1 and one for the terminal segment S_2. For the case of the semicircle part, the angle φ from the x-axis can be expressed as

$$\varphi = \theta \pm \arccos\frac{p}{a}. \tag{5.5}$$

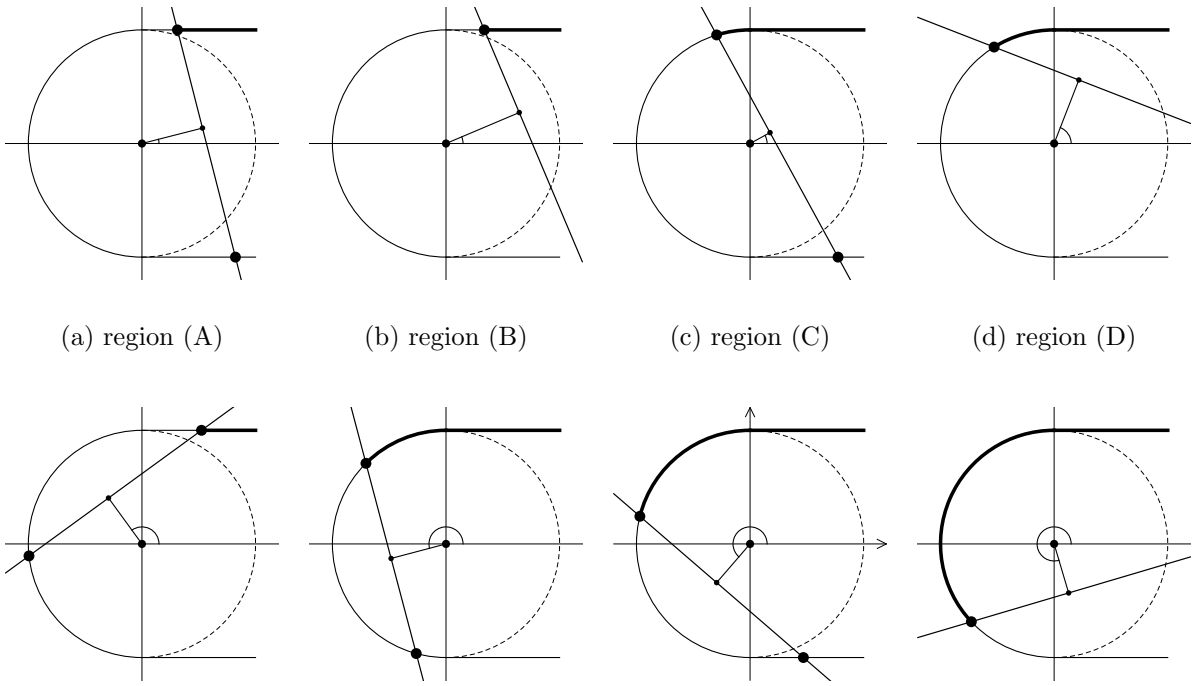

(a) region (A) (b) region (B) (c) region (C) (d) region (D)

(e) region (E) (f) region (F) (g) region (G) (h) region (H)

(i) region (I) (j) region (J) (k) region (K)

Figure 6: Intersection patterns of a cable and the U-shape

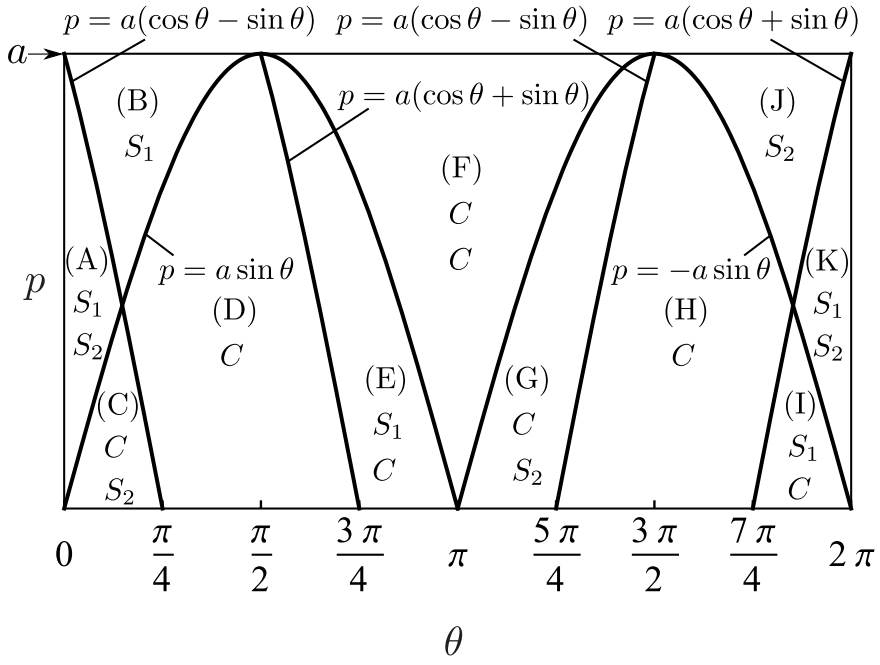

Figure 7: Division of region R into sub-regions by intersection pattern (U-model)

For the case of segments S_1: $(y = a) \cap (0 \le x \le a)$ and S_2: $(y = -a) \cap (0 \le x \le a)$, we can obtain expressions for the coordinates as

$$S_1 : \left(\frac{p - a\sin\theta}{\cos\theta}, a \right), \tag{5.6}$$

$$S_2 : \left(\frac{p + a\sin\theta}{\cos\theta}, -a \right) \tag{5.7}$$

by focusing on the fact that the cable can be characterized by

$$p = x\cos\theta + y\sin\theta. \tag{5.8}$$

Since the intersection point that a trench digger finds is one of the above four cases, the trench length L_{U} can be obtained as follows:

(i) (A), (B), (E), (I) and (K)

$$L_{\mathrm{U}} = a - \frac{p - a\sin\theta}{\cos\theta}, \tag{5.9}$$

(ii) (C) and (D)

$$L_{\mathrm{U}} = a + a\left(\theta + \arccos\frac{p}{a} - \frac{\pi}{2}\right), \tag{5.10}$$

(iii) (F), (G) and (H)

$$L_{\mathrm{U}} = a + a\left(\theta - \arccos\frac{p}{a} - \frac{\pi}{2}\right), \tag{5.11}$$

(iv) (J)

$$L_{\mathrm{U}} = a + \pi a + \frac{p + a\sin\theta}{\cos\theta}. \tag{5.12}$$

To derive $F_{L_{\mathrm{U}}}(l)$, the cdf of the trench length, we have to identify the region $\Omega_{\mathrm{U}}(l)$ in the region R that satisfies the condition $L_{\mathrm{U}} \leq l$. $F_{L_{\mathrm{U}}}(l)$ can be expressed as follows:

$$F_{L_{\mathrm{U}}}(l) = \iint_{\Omega_{\mathrm{U}}(l)} f_{\Theta,P}(\theta, p)\mathrm{d}\theta\mathrm{d}p. \tag{5.13}$$

It should be noted that the shape of $\Omega_{\mathrm{U}}(l)$ changes depending on the value of l, where $l \in [0, (\pi+2)a]$. For more detailed process for deriving the cdf, see the appendix B.

Under the uniformity assumption of Equation (3.2), the cdf can be derived as follows:

(i) $0 \leq l \leq a$

$$F_{L_{\mathrm{U}}}(l) = \frac{1}{2\pi}\arccos\left(\frac{2a^2 - 2al}{2a^2 - 2al + l^2}\right), \tag{5.14}$$

(ii) $a \leq l \leq (\pi+1)a$

$$F_{L_{\mathrm{U}}}(l) = \frac{1}{2\pi}\left\{\frac{l}{a} + \frac{\pi}{2} - 2 + \sqrt{2\sin\left(\tfrac{l-a}{a}\right) - 2\cos\left(\tfrac{l-a}{a}\right) + 3}\right\}, \tag{5.15}$$

(iii) $(\pi+1)a \leq l \leq (\pi+2)a$

$$F_{L_{\mathrm{U}}}(l) = \frac{1}{2\pi}\left\{3\pi - \frac{l}{a} + \sqrt{4 + \left(\pi + 2 - \tfrac{l}{a}\right)^2} - \arccos\left(\tfrac{2al - (2+2\pi)a^2}{(\pi^2+2\pi+2)a^2 - 2(\pi+1)al + l^2}\right)\right\}. \tag{5.16}$$

By differentiating Equations (5.14)–(5.16) with respect to l, the pdf $f_{L_{\mathrm{U}}}(l)$ of trench length can be derived as follows:

(i) $0 \leq l \leq a$

$$f_{L_{\mathrm{U}}}(l) = \frac{a}{\pi\{a^2 + (l-a)^2\}}, \tag{5.17}$$

(ii) $a \leq l \leq (\pi+1)a$

$$f_{L_{\mathrm{U}}}(l) = \frac{1}{2\pi a}\left\{\frac{\sin\left(\tfrac{l-a}{a}\right) + \cos\left(\tfrac{l-a}{a}\right)}{\sqrt{2\sin\left(\tfrac{l-a}{a}\right) - 2\cos\left(\tfrac{l-a}{a}\right) + 3}} + 1\right\}, \tag{5.18}$$

(iii) $(\pi+1)a \leq l \leq (\pi+2)a$

$$f_{L_{\mathrm{U}}}(l) = \frac{1}{2\pi a}\left\{\frac{2a^2}{a^2 + \{l - (\pi+1)a\}^2} - \frac{(\pi+2)a - l}{\sqrt{4a^2 + \{(\pi+2)a - l\}^2}} - 1\right\}. \tag{5.19}$$

Since analytical derivation of the expected value of the trench length $\mathrm{E}[L_{\mathrm{U}}]$ and the variance $\mathrm{Var}[L_{\mathrm{U}}]$, is difficult, we evaluate these values by numerical integration. The following are approximate values of $\mathrm{E}[L_{\mathrm{U}}]$ and $\mathrm{Var}[L_{\mathrm{U}}]$ obtained by Wolfram Mathematica 10 (`http://www.wolfram.com`).

$$\mathrm{E}[L_{\mathrm{U}}] = \int_0^{(\pi+2)a} l f_{L_{\mathrm{U}}}(l)\mathrm{d}l \approx 1.966a, \tag{5.20}$$

$$\mathrm{Var}[L_{\mathrm{U}}] = \int_0^{(\pi+2)a} (l - \mathrm{E}[L_{\mathrm{U}}])^2 f_{L_{\mathrm{U}}}(l)\mathrm{d}l \approx 1.418a^2. \tag{5.21}$$

This result illustrates an interesting fact: The expected value of the trench length for the U-model is about 5% longer than that for the O-model as derived in Equation (4.10).

6. Comparison of Two Models

We compare the two models on the basis of the results derived in the two preceding sections. Figure 8 compares the cdfs of the O-model (thinner line) and the U-model (thicker line) for $a = 1$. Figure 9 shows the pdfs of the two models. We also present summary values (expected values, maximum values, and variances) in Table 1.

As can be seen from Figure 8, the cdf of the O-model (thinner line) is larger than that of the U-model (thicker line) for smaller values of l. This fact can also be seen from Figure 9. As presented in Equation (4.9), the pdf of the O-model is given by the simple cosine curve, which decreases monotonically. In contrast, the pdf of the U-model has a peak at a. For smaller l, the probability of finding a trench in the O-model is much larger than in the U-model. In fact, it can be easily shown that the pdf for the O-model at $l = 0$ is twice that of the U-model at $l = 0$:

$$f_{L_{\mathrm{O}}}(0) = \frac{1}{\pi a}, \tag{6.1}$$

$$f_{L_{\mathrm{U}}}(0) = \frac{1}{2\pi a}. \tag{6.2}$$

Note that the expected value of the trench length of the O-model is about 5% less than that of the U-model. Earlier studies have focused on only the maximum trench length (i.e., the worst-case scenario) and have concluded that the U-method is the best method among those employing a single simply connected curve. Using our results, it is interesting to compare O- and U-models from a similar pessimistic viewpoint, as in the literature [5]. It can be easily derived that the probability of a trench digger having to dig a longer trench under the O-method than the maximum trench length of the U-method is given as follows:

$$\Pr\{L_{\mathrm{O}} \geq (\pi+2)a\} = \int_{(\pi+2)a}^{2\pi a} f_{L_{\mathrm{O}}}(l)\mathrm{d}l = \frac{\pi - 2 - 2\cos(1)}{2\pi} \approx 0.0097. \tag{6.3}$$

Interestingly, this probability is less than 1%. This result suggests that the circular trench may be a better choice than the U-shaped trench, except when it is crucial to avoid the worst-case trench length.

Lastly, in terms of the variance of the trench length, the U-method, which has smaller value than the other, is superior to that of the O-method.

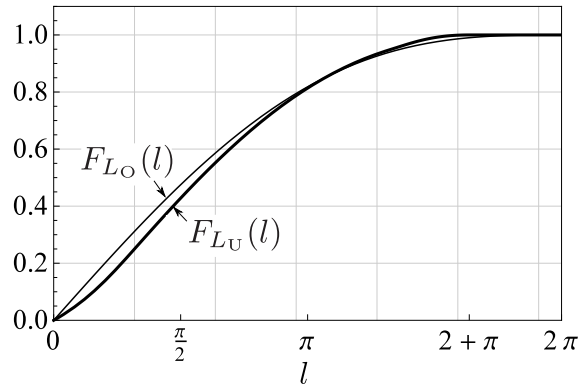

Figure 8: Cumulative distribution functions of O-model and U-model ($a = 1$)

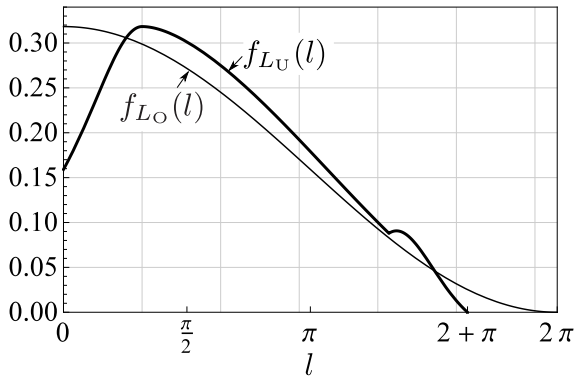

Figure 9: Probability density functions of O-model and U-model ($a = 1$)

Table 1: Summary values of O-model and U-model

	O-model	U-model
Expected value	$1.868a$	$1.966a$
Maximum value	$6.283a$	$5.142a$
Variance	$1.669a^2$	$1.418a^2$

7. Conclusions and Future Research Perspectives

This paper focused on mathematical models proposed by Faber et al. [5] that deal with efficient methods for finding a buried cable. The problem is to find the shortest simply connected curve that ensures finding a cable when a trench digger searches along it to locate the intersection point between a cable and the curve. Faber et al. [4] proved the very interesting fact that the U-shape is the shortest single-curve simply connected trench. This problem can be seen as finding a curve that minimizes the maximum trench length that a trench digger must search.

While the above results are very interesting mathematically, the maximum value is only one of the many important indices in real applications. In reality an important fact is that once a cable is found, a trench digger can stop searching. Thus, in this paper, we constructed a probabilistic model that describes random realization of a cable. Using the probabilistic model, we succeeded in obtaining analytical expressions of the cdfs and the pdfs of the O- and U-models. One of our main results is that although the U-model is superior to the O-model in terms of the maximum trench length, as proved by Faber et al. [4], the O-model is more than 5% better than U-model in terms of the expected value of trench length.

To our knowledge, our results are the first to analytically derive measures other than the maximum necessary trench. The approach taken in this paper can be extended in a wide variety of directions. We mention some of them in the following.

This paper modeled the realization of a cable using random lines. While this is the most important basic case, other possibilities may be considered. One important case is that the probability of finding a cable locations closer to the marker is higher than that at more remote locations. This situation may be described by assuming that $f_P(p)$ is a monotonically decreasing function of p. This case can be readily dealt with using formulations presented in the Appendix. In urban applications, some line-shaped network facilities such as water and sewer networks are buried under road segment. Thus, another possibility is to consider the situation where the probability of finding a cable running in a particular direction may

be higher than finding one running in other directions.

Next, relaxing the assumption that a trench digger moves continuously along the predefined continuous curve may be an interesting topic to explore. In reality, a trench digger may evaluate the probability of finding a cable for each part of the curve and may start search for the cable from the part with the highest probability. Since this approach is more flexible, a trench digger may find the cable in a smaller amount of time than suggested by the approach taken in this paper. However, in such situations, the costs of stopping and restarting digging cannot be ignored. Therefore, we can extend the original problem by incorporating this cost into the time required to find a cable.

We focused on the pdfs and expected trench lengths obtained for two strategies of finding a cable. The problem formulation naturally leads to the following interesting, but challenging, question. What trench shape is best in terms of the minimum expected length to find a cable?

Acknowledgements

The authors would like to thank two anonymous referees for their constructive comments and suggestions. This work was supported by JSPS KAKENHI Grant Number JP25242029.

References

[1] H.T. Croft: Curves intersecting certain sets of great-circles on the sphere. *Journal of the London Mathematical Society*, **2** (1969), 461–469.

[2] H.T. Croft, K.J. Falconer, and R.K. Guy: *Unsolved Problems in Geometry* (Springer, New York, 1991).

[3] A. Dumitrescu, M. Jiang, and J. Pach: Opaque sets. *Algorithmica*, **69** (2014), 315–334.

[4] V. Faber, J. Mycielski, and P. Pedersen: On the shortest curve which meets all lines which meet a circle. *Annales Polonici Mathematici*, **44** (1984), 249–266.

[5] V. Faber and J. Mycielski: The shortest curve that meets all lines that meet a convex body. *American Mathematical Monthly*, **93** (1986), 796–801.

[6] S.R. Finch: Beam detection constant. In *Mathematical Constants* (Cambridge University Press, Cambridge, 2003), 515–519.

[7] S.R. Finch and J.E. Wetzel: Lost in a forest. *American Mathematical Monthly*, **111** (2004), 645–654.

[8] B. Kawohl: Some nonconvex shape optimization problems. In A. Cellina and A. Ornelas (eds.): *Optimal Shape Design*, Lecture Notes in Mathematics (Springer, New York, 2000), 7–46.

[9] T. Koshizuka: Distance distribution in an urban area. In H. Tanimura, H. Kaji, S. Ikeda, and T. Koshizuka (eds.): *Mathematical Methods in Urban Planning* (Asakura Publishing, Tokyo, 1986), 1–55 (in Japanese).

[10] P.J. Nahin: *When Least is Best: How Mathematicians Discovered Many Clever Ways to Make Things as Small (or as Large) as Possible* (Princeton University Press, New Jersey, 2007).

[11] A.M. Mathai: *An Introduction to Geometrical Probability: Distributional Aspects with Applications* (Gordon and Breach Science Publishers, Amsterdam, 1999).

[12] L.A. Santalo: *Integral Geometry and Geometric Probability*, 2nd Edition (Cambridge University Press, Cambridge, 2004).

[13] H. Solomon: *Geometric Probability* (SIAM, Philadelphia, 1978).

[14] I. Stewart: The great drain robbery. *Scientific American*, **273** (1995), 206–207.
[15] R.C. Larson and A.R. Odoni: *Urban Operations Research* (Prentice Hall, New Jersey, 1981).
[16] R.J. Vaughan: *Urban Spatial Traffic Patterns* (Pion, London, 1987).

Appendix A: Derivation of $F_{L_O}(l)$

To derive the cdf of the trench length $F_{L_O}(l)$, we have to identify how $\Omega_O(l)$ changes according to the value of l. As shown in Figure 10, there are three different shapes of $\Omega_O(l)$: (I), (II) and (III). In the Figures, the vertical hatched areas, the horizontal hatched areas and the meshed areas correspond to the set of points (θ, p) in which the trench lengths are given by Equation (4.4), Equation (4.5) and Equation (4.6), respectively.

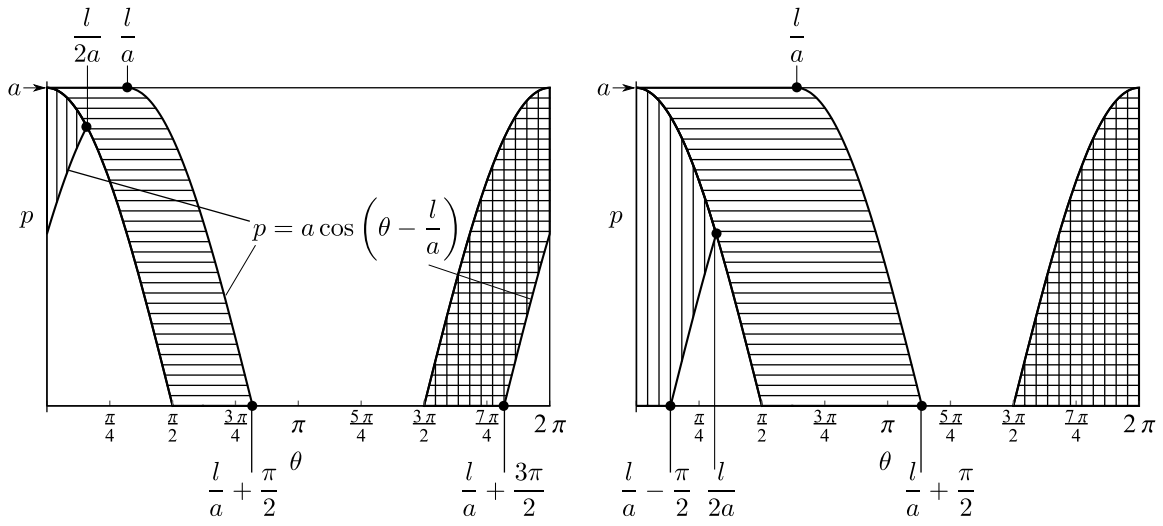

(a) case (I)

(b) case (II)

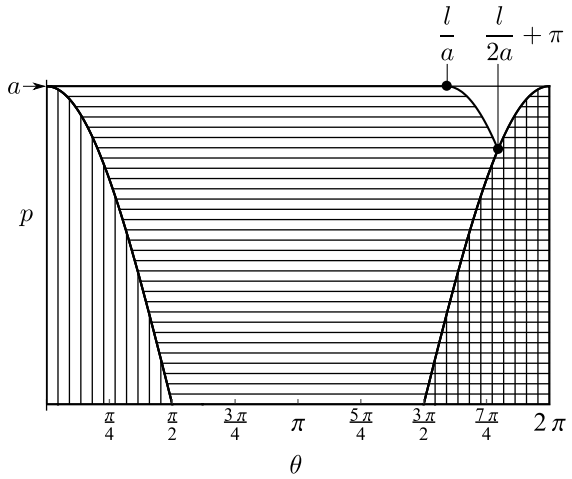

(c) case (III)

Figure 10: Three different shapes of $\Omega_O(l)$

For cases (I), (II) and (III), $F_{L_O}(l)$ can be expressed as follows:

(I) $0 \le l \le \frac{\pi}{2}a$

$$\begin{aligned}F_{L_{\mathrm{O}}}(l) = &\int_0^{\frac{l}{2a}} \int_{a\cos\left(\theta-\frac{l}{a}\right)}^{a} f_{\Theta,P}(\theta,p)\mathrm{d}p\mathrm{d}\theta + \int_{\frac{l}{2a}}^{\frac{l}{a}} \int_{a\cos\theta}^{a} f_{\Theta,P}(\theta,p)\mathrm{d}p\mathrm{d}\theta \\ &+ \int_{\frac{l}{a}}^{\frac{\pi}{2}} \int_{a\cos\theta}^{a\cos\left(\theta-\frac{l}{a}\right)} f_{\Theta,P}(\theta,p)\mathrm{d}p\mathrm{d}\theta + \int_{\frac{\pi}{2}}^{\frac{l}{a}+\frac{\pi}{2}} \int_{0}^{a\cos\left(\theta-\frac{l}{a}\right)} f_{\Theta,P}(\theta,p)\mathrm{d}p\mathrm{d}\theta \\ &+ \int_{\frac{3\pi}{2}}^{\frac{l}{a}+\frac{3\pi}{2}} \int_{0}^{a\cos\theta} f_{\Theta,P}(\theta,p)\mathrm{d}p\mathrm{d}\theta + \int_{\frac{l}{a}+\frac{3\pi}{2}}^{2\pi} \int_{a\cos\left(\theta-\frac{l}{a}\right)}^{a\cos\theta} f_{\Theta,P}(\theta,p)\mathrm{d}p\mathrm{d}\theta, \end{aligned} \tag{A.1}$$

(II) $\frac{\pi}{2}a \le l \le \pi a$

$$\begin{aligned}F_{L_{\mathrm{O}}}(l) = &\int_0^{\frac{l}{a}-\frac{\pi}{2}} \int_{0}^{a} f_{\Theta,P}(\theta,p)\mathrm{d}p\mathrm{d}\theta + \int_{\frac{l}{a}-\frac{\pi}{2}}^{\frac{l}{2a}} \int_{a\cos\left(\theta-\frac{l}{a}\right)}^{a} f_{\Theta,P}(\theta,p)\mathrm{d}p\mathrm{d}\theta \\ &+ \int_{\frac{l}{2a}}^{\frac{\pi}{2}} \int_{a\cos\theta}^{a} f_{\Theta,P}(\theta,p)\mathrm{d}p\mathrm{d}\theta + \int_{\frac{\pi}{2}}^{\frac{l}{a}} \int_{0}^{a} f_{\Theta,P}(\theta,p)\mathrm{d}p\mathrm{d}\theta \\ &+ \int_{\frac{l}{a}}^{\frac{l}{a}+\frac{\pi}{2}} \int_{0}^{a\cos\left(\theta-\frac{l}{a}\right)} f_{\Theta,P}(\theta,p)\mathrm{d}p\mathrm{d}\theta + \int_{\frac{3\pi}{2}}^{2\pi} \int_{0}^{a\cos\theta} f_{\Theta,P}(\theta,p)\mathrm{d}p\mathrm{d}\theta, \end{aligned} \tag{A.2}$$

(III) $\pi a \le l \le 2\pi a$

$$\begin{aligned}F_{L_{\mathrm{O}}}(l) = &\int_0^{\frac{l}{a}} \int_{0}^{a} f_{\Theta,P}(\theta,p)\mathrm{d}p\mathrm{d}\theta + \int_{\frac{l}{a}}^{\frac{l}{2a}+\pi} \int_{0}^{a\cos\left(\theta-\frac{l}{a}\right)} f_{\Theta,P}(\theta,p)\mathrm{d}p\mathrm{d}\theta \\ &+ \int_{\frac{l}{2a}+\pi}^{2\pi} \int_{0}^{a\cos\theta} f_{\Theta,P}(\theta,p)\mathrm{d}p\mathrm{d}\theta. \end{aligned} \tag{A.3}$$

Appendix B: Derivation of $F_{L_{\mathrm{U}}}(l)$

The process of deriving the cdf, $F_{L_{\mathrm{U}}}(l)$, is basically the same as that of $F_{L_{\mathrm{O}}}(l)$. However, identifying $\Omega_{\mathrm{U}}(l)$ for all possible cases is much more complicated than that of $\Omega_{\mathrm{O}}(l)$ due to the lower symmetry of the U-shape. As shown in Figure 11, there are five different shapes of $\Omega_{\mathrm{U}}(l)$: (I), (II), (III), (IV) and (V). In the Figures, the vertical hatched areas, the horizontal hatched areas, the meshed areas and the gray areas correspond to the set of points (θ, p) in which the trench lengths are given by Equation (5.9), Equation (5.10), Equation (5.11) and Equation (5.12), respectively.

For cases (I), (II), (III), (IV) and (V), $F_{L_{\mathrm{U}}}(l)$ can be expressed as follows:

(I) $0 \le l \le a$

$$\begin{aligned}F_{L_{\mathrm{U}}}(l) = &\int_0^{\arccos\left\{\frac{2a(a-l)}{a^2+(a-l)^2}\right\}} \int_{a\sin\theta+(a-l)\cos\theta}^{a} f_{\Theta,P}(\theta,p)\mathrm{d}p\mathrm{d}\theta + \int_{\frac{\pi}{2}}^{\frac{3\pi}{4}} \int_{a(\cos\theta+\sin\theta)}^{a\sin\theta+(a-l)\cos\theta} f_{\Theta,P}(\theta,p)\mathrm{d}p\mathrm{d}\theta \\ &+ \int_{\frac{3\pi}{4}}^{\pi-\arctan\left(1-\frac{l}{a}\right)} \int_{0}^{a\sin\theta+(a-l)\cos\theta} f_{\Theta,P}(\theta,p)\mathrm{d}p\mathrm{d}\theta + \int_{\frac{7\pi}{4}}^{2\pi-\arctan\left(1-\frac{l}{a}\right)} \int_{0}^{a(\cos\theta+\sin\theta)} f_{\Theta,P}(\theta,p)\mathrm{d}p\mathrm{d}\theta \\ &+ \int_{2\pi-\arctan\left(1-\frac{l}{a}\right)}^{2\pi} \int_{a\sin\theta+(a-l)\cos\theta}^{a(\cos\theta+\sin\theta)} f_{\Theta,P}(\theta,p)\mathrm{d}p\mathrm{d}\theta, \end{aligned} \tag{B.1}$$

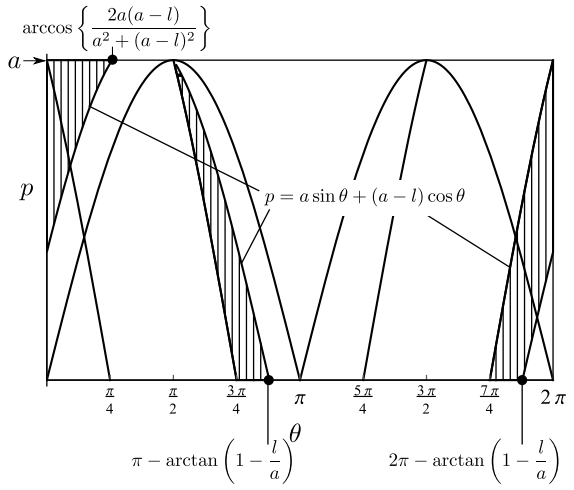

(a) case (I)

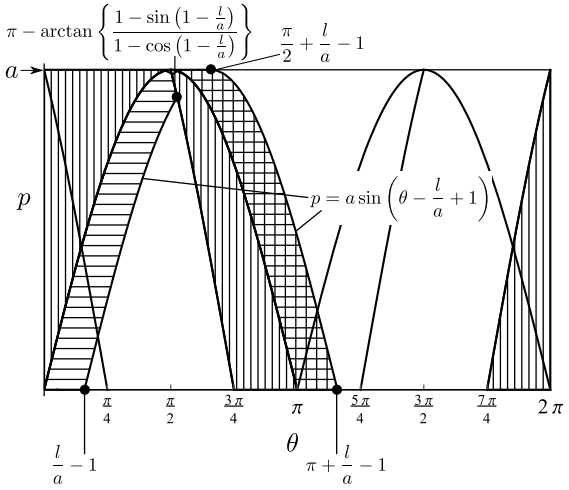

(b) case (II)

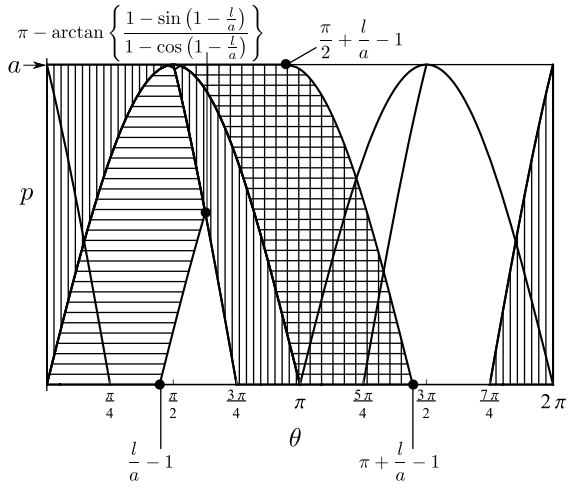

(c) case (III)

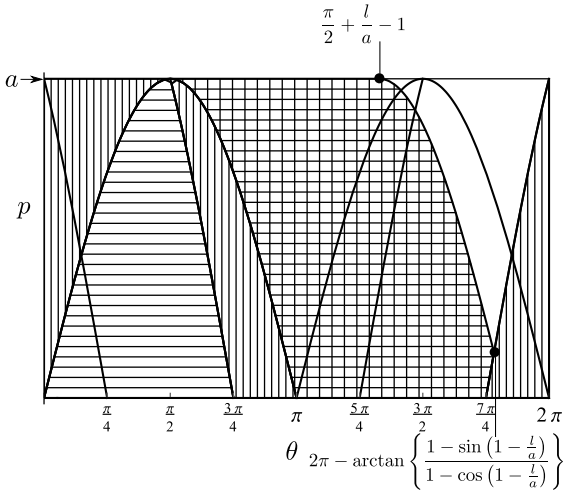

(d) case (IV)

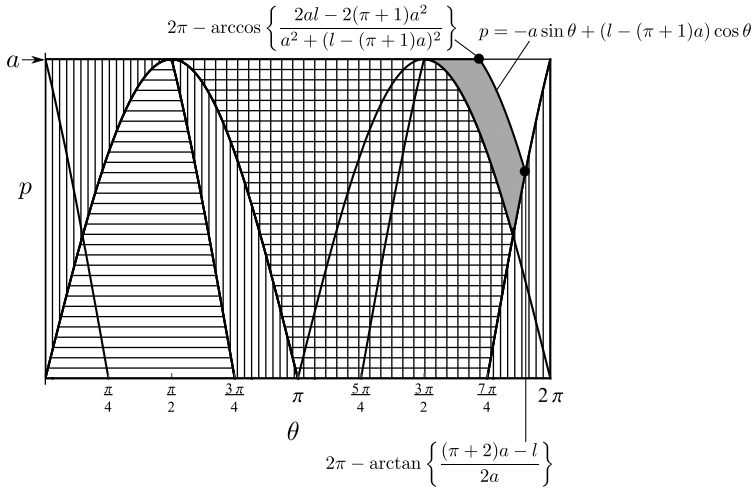

(e) case (V)

Figure 11: Five different shapes of $\Omega_{\mathrm{U}}(l)$

(II) $a \leq l \leq \left(\frac{\pi}{4}+1\right)a$

$$F_{L_{\mathrm{U}}}(l) = \int_0^{\frac{l}{a}-1}\int_0^{a} f_{\Theta,P}(\theta,p)\mathrm{d}p\mathrm{d}\theta + \int_{\frac{l}{a}-1}^{\pi-\arctan\left\{\frac{1-\sin\left(1-\frac{l}{a}\right)}{1-\cos\left(1-\frac{l}{a}\right)}\right\}}\int_{a\sin\left(\theta-\frac{l}{a}+1\right)}^{a} f_{\Theta,P}(\theta,p)\mathrm{d}p\mathrm{d}\theta$$
$$+ \int_{\pi-\arctan\left\{\frac{1-\sin\left(1-\frac{l}{a}\right)}{1-\cos\left(1-\frac{l}{a}\right)}\right\}}^{\frac{\pi}{2}+\frac{l}{a}-1}\int_{a(\sin\theta+\cos\theta)}^{a} f_{\Theta,P}(\theta,p)\mathrm{d}p\mathrm{d}\theta + \int_{\frac{\pi}{2}+\frac{l}{a}-1}^{\frac{3\pi}{4}}\int_{a(\sin\theta+\cos\theta)}^{a\sin\left(\theta-\frac{l}{a}+1\right)} f_{\Theta,P}(\theta,p)\mathrm{d}p\mathrm{d}\theta$$
$$+ \int_{\frac{3\pi}{4}}^{\pi+\frac{l}{a}-1}\int_{0}^{a\sin\left(\theta-\frac{l}{a}+1\right)} f_{\Theta,P}(\theta,p)\mathrm{d}p\mathrm{d}\theta + \int_{\frac{7\pi}{4}}^{2\pi}\int_{0}^{a(\sin\theta+\cos\theta)} f_{\Theta,P}(\theta,p)\mathrm{d}p\mathrm{d}\theta, \tag{B.2}$$

(III) $\left(\frac{\pi}{4}+1\right)a \leq l \leq \left(\frac{3\pi}{4}+1\right)a$

$$F_{L_{\mathrm{U}}}(l) = \int_0^{\frac{l}{a}-1}\int_0^{a} f_{\Theta,P}(\theta,p)\mathrm{d}p\mathrm{d}\theta + \int_{\frac{l}{a}-1}^{\pi-\arctan\left\{\frac{1-\sin\left(1-\frac{l}{a}\right)}{1-\cos\left(1-\frac{l}{a}\right)}\right\}}\int_{a\sin\left(\theta-\frac{l}{a}+1\right)}^{a} f_{\Theta,P}(\theta,p)\mathrm{d}p\mathrm{d}\theta$$
$$+ \int_{\pi-\arctan\left\{\frac{1-\sin\left(1-\frac{l}{a}\right)}{1-\cos\left(1-\frac{l}{a}\right)}\right\}}^{\frac{3\pi}{4}}\int_{a(\sin\theta+\cos\theta)}^{a} f_{\Theta,P}(\theta,p)\mathrm{d}p\mathrm{d}\theta + \int_{\frac{3\pi}{4}}^{\frac{\pi}{2}+\frac{l}{a}-1}\int_{0}^{a} f_{\Theta,P}(\theta,p)\mathrm{d}p\mathrm{d}\theta$$
$$+ \int_{\frac{\pi}{2}+\frac{l}{a}-1}^{\pi+\frac{l}{a}-1}\int_{0}^{a\sin\left(\theta-\frac{l}{a}+1\right)} f_{\Theta,P}(\theta,p)\mathrm{d}p\mathrm{d}\theta + \int_{\frac{7\pi}{4}}^{2\pi}\int_{0}^{a(\sin\theta+\cos\theta)} f_{\Theta,P}(\theta,p)\mathrm{d}p\mathrm{d}\theta, \tag{B.3}$$

(IV) $\left(\frac{3\pi}{4}+1\right)a \leq l \leq (\pi+1)a$

$$F_{L_{\mathrm{U}}}(l) = \int_0^{\frac{\pi}{2}+\frac{l}{a}-1}\int_0^{a} f_{\Theta,P}(\theta,p)\mathrm{d}p\mathrm{d}\theta + \int_{\frac{\pi}{2}+\frac{l}{a}-1}^{2\pi-\arctan\left\{\frac{1-\sin\left(1-\frac{l}{a}\right)}{1-\cos\left(1-\frac{l}{a}\right)}\right\}}\int_{0}^{a\sin\left(\theta-\frac{l}{a}+1\right)} f_{\Theta,P}(\theta,p)\mathrm{d}p\mathrm{d}\theta$$
$$+ \int_{2\pi-\arctan\left\{\frac{1-\sin\left(1-\frac{l}{a}\right)}{1-\cos\left(1-\frac{l}{a}\right)}\right\}}^{2\pi}\int_{0}^{a(\sin\theta+\cos\theta)} f_{\Theta,P}(\theta,p)\mathrm{d}p\mathrm{d}\theta, \tag{B.4}$$

(V) $(\pi+1)a \leq l \leq (\pi+2)a$

$$F_{L_{\mathrm{U}}}(l) = \int_0^{2\pi-\arccos\left\{\frac{2al-2(\pi+1)a^2}{a^2+(l-(\pi+1)a)^2}\right\}}\int_0^{a} f_{\Theta,P}(\theta,p)\mathrm{d}p\mathrm{d}\theta$$
$$+ \int_{2\pi-\arccos\left\{\frac{2al-2(\pi+1)a^2}{a^2+(l-(\pi+1)a)^2}\right\}}^{2\pi-\arctan\left\{\frac{(\pi+2)a-l}{2a}\right\}}\int_{0}^{-a\sin\theta+(l-(\pi+1)a)\cos\theta} f_{\Theta,P}(\theta,p)\mathrm{d}p\mathrm{d}\theta$$
$$+ \int_{2\pi-\arctan\left\{\frac{(\pi+2)a-l}{2a}\right\}}^{2\pi}\int_{0}^{a(\sin\theta+\cos\theta)} f_{\Theta,P}(\theta,p)\mathrm{d}p\mathrm{d}\theta. \tag{B.5}$$

Ken-ichi Tanaka
Keio University
3-14-1 Hiyoshi, Kohoku-ku, Yokohama
Kanagawa 223-8522, Japan
E-mail: ken1tnk@ae.keio.ac.jp